

Preparation of Nb₂O₅ Coated TiO₂ Nanoporous Electrodes and Their Application in Dye-Sensitized Solar Cells

S. G. Chen, S. Chappel, Y. Diamant, and A. Zaban*

Department of Chemistry, Bar-Ilan University, Ramat-Gan, 52900, Israel

Received April 19, 2001. Revised Manuscript Received September 13, 2001

The preparation of a new bilayer nanoporous wide band gap semiconductor electrode and its application for solar cells are reported. This new electrode consists of an inner nanoporous TiO₂ matrix covered with a thin layer of ca. 2–3 nm Nb₂O₅. The results presented in this study show that this Nb₂O₅ layer forms an inherent energy barrier at the electrode–electrolyte interface. This barrier reduces the recombination rate of the photoinjected electrons with their counter holes. A comparison of two similar dye-sensitized solar cells (DSSCs) that differ only in their nanoporous electrodes shows that the solar cells made from the new electrode are superior to the standard cells with respect to all parameters. This superiority measured with many cells results in a 35% increase of the overall conversion efficiency from 3.6 to 5.0%. Optimization of the coating process and the characterization of the coating effects are described.

Introduction

From the time DSSCs were first reported in the literature, they were considered attractive for light-to-energy conversion applications because of their relatively low cost and efficiency as high as 11%.¹ This high efficiency of dye-sensitized solar cells (DSSCs) was achieved only when the nanoporous TiO₂ electrodes² were introduced, thus enabling high optical density of a dye monolayer. The electrodes consist of nanosize semiconductor colloids that are sintered on a transparent conducting substrate, resulting in a porous geometry and a very large surface area. However, the resulting electrode geometry introduces special characteristics, some of which reduce the performance of the DSSCs.^{3–5} One of these characteristics relates to the small size of the individual colloidal particles that cannot support a high space charge.^{3,5,6} In other words, an energy barrier is not formed at the electrode–electrolyte interface.

Upon illumination of a DSSC, an electron is injected from the dye into the TiO₂ film followed by a hole transfer to the electrolyte.^{1,2} The injected electrons must cross the TiO₂ film and reach the conducting substrate, while the oxidized ions diffuse toward the back electrode where they are reduced again. The porous geometry that permits the presence of the electrolyte through the

entire electrode provides a high surface area for recombination between the injected electrons and the holes in the solution.^{3,7} In the absence of an energy barrier at the electrode–electrolyte interface, the rate of this recombination process may be very high, depending on the properties of the hole carrier.^{1,3,8,9} For this reason, DSSCs using the I⁻/I₃⁻ redox couple perform better than similar cells consisting of faster couples.¹⁰ Furthermore, part of the low efficiencies observed with solid electrolytes is attributed to this recombination process. Therefore, the formation of an energy barrier at the surface of the TiO₂ electrode that will enable the use of various mediators has the prospect of improving DSSCs significantly.

In our previous communication,¹¹ we reported a new type of electrode having an intrinsic energy barrier. This new electrode consists of an inner nanoporous TiO₂ matrix covered with a thin layer of Nb₂O₅. The conduction band potential difference of Nb₂O₅ is ca. 100 mV more negative than that of TiO₂.¹² This potential difference can form an energy barrier at the electrode–electrolyte interface thus reducing the rate of recombination of the photoinjected electrons and improving the collection efficiency.¹¹ A comparison of two similar DSSCs that differ only in their nanoporous electrodes shows that the solar cells made from the new electrode are superior to cells containing the standard electrodes with respect to all parameters. The overall conversion

* To whom correspondence should be addressed. Tel: +972–3–5317876. Fax: +972–3–5351250. E-mail: zabana@mail.biu.ac.il.

(1) O'Regan, B.; Gratzel, M. *Nature* **1991**, *353*, 347.
(2) Kalyanasundaram, K.; Gratzel, M. *Coord. Chem. Rev.* **1998**, *77*, 347.
(3) Hagfeldt, A.; Lindquist, S. E.; Gratzel, M. *Sol. Energy Mater. Sol. Cells* **1994**, *32*, 245.
(4) Zaban, A.; Meier, A.; Gregg, B. A. *J. Phys. Chem. B* **1997**, *101*, 7985.
(5) Bisquert, J.; Garcia-Belmonte, G.; Fabregat-Santiago, F. *J. Solid State Electrochem.* **1999**, *3*, 337.
(6) Kavan, L.; Gratzel, M.; Gilbert, S. E.; Klemenz, C.; Scheel, H. *J. Am. Chem. Soc.* **1996**, *118*, 6716.

(7) Tachibana, Y.; Moser, J. E.; Gratzel, M.; Klug, D.; Durrant, J. R. *J. Phys. Chem. B* **1996**, *100*, 20056.

(8) Bedja, I.; Hotchandani, S.; Kamat, P. V. *Ber. Bunsen-Ges. Phys. Chem. Chem. Phys.* **1997**, *101*, 1651.

(9) Nasr, C.; Kamat, P. V.; Hotchandani, S. *J. Electroanal. Chem.* **1997**, *420*, 201.

(10) Pichot, F.; Gregg, B. A. *J. Phys. Chem. B* **2000**, *104*, 6.

(11) Zaban, A.; Chen, S. G.; Chappel, S.; Gregg, B. A. *Chem. Commun.* **2000**, 2231.

(12) Sayama, K.; Sugihara, H.; Arakawa, H. *Chem. Mater.* **1998**, *10*, 3825.

efficiency increased from 3.6 to 5.0% corresponding to a 35% improvement of the cell performance. We report here on details of the preparation of this type of electrode, the optimization methods, the characterization of the electrode, and further evidence of the role of the coating in the electrode's electrochemical behavior.

Experimental Section

Materials and Methods. Niobium(V) chloride (99.9%), Niobium(V) isopropoxide (99%), and Niobium(V) ethoxide (99.99%) were purchased from Chemical Technology, Inc. The remaining chemical materials were purchased from Aldrich Chemical Co. and used as received. The dye [cis-di(isothiocyanato)-bis(4,4'-dicarboxy-2,2'-bipyridine) ruthenium (II)] (N3) was purchased from Solaronix SA Co.

Conducting glass substrate (Libby Owens Ford) with 8 Ohm/square F-doped SnO₂ was cleaned with soap, rinsed with deionized water (18.2 MΩ), and dried in a nitrogen stream.

The thickness of the TiO₂ films was measured with a SurfTest SV 500 profilometer of Mitutoyo Co. Absorption spectra were recorded using a HP 8453 spectrophotometer. Kratos Analytical X-ray Photoelectron Spectrum was used to investigate the quality of the Nb₂O₅ coating and to estimate the thickness of the coating layer. A Bruker D8 X-ray diffractometer was used to measure the crystalline structure change of TiO₂ films due to the Nb₂O₅ coating and to study the matching between the crystalline plane of the TiO₂ and the Nb₂O₅.

Preparation of TiO₂ and Nb₂O₅ Coated TiO₂ Electrodes. The TiO₂ slurries, consisting of 23-nm-sized particles characterized by XRD and TEM, were prepared by hydrolyzing titanium tetraisopropoxide in acetic acid pH 2 solution. After overnight stirring, the solution was evaporated at 82 °C followed by autoclaving at 250 °C for 13 h.¹³ The resulting suspension was spread on the substrates by a glass rod, using adhesive tapes as spacers. After the films dried in air, they were sintered at 450 °C for 30 min in air. The thickness of the TiO₂ films was controlled using different tape and thickness between 2 and 6 μm.

After sintering, the TiO₂ matrixes were coated with Nb₂O₅ by dipping a coating in solutions of various niobium precursor solutions followed by oxidation. The dipping procedures differ by the niobium compounds, concentration, dipping time, and number of layers. We also tested other coating types such as spin coating. The coating with a precursor was prepared under dry nitrogen atmosphere, followed by sintering at 500 °C for 30 min in air. To keep the similar conditions between the standard and coated electrodes, the TiO₂ films without Nb₂O₅ coating were also sintered with the coated ones. The niobium precursors used in this work include: Niobium(V) chloride, Niobium(V) isopropoxide, and Niobium(V) ethoxide, which were dissolved in dry ethanol or 2-propanol.

The N3 used to sensitize the electrodes was adsorbed by immersing the electrodes in a 0.5 mM solution of dye in absolute ethanol overnight. To avoid water, the films were heated to 150 °C and cooled to 80 °C before immersion in the dye solution. The oxidation potential of the dye (ca. 1.09 V vs NHE in acetonitrile) is sufficient to allow injection into both TiO₂ and Nb₂O₅. The electrodes were kept in the dye solution until the measurement in the dye-sensitized solar cells was performed.

Electrochemical and Photoelectrochemical Measurements. A sandwich-type configuration was employed to measure the performance of the dye-sensitized solar cell, using a Pt coated F-doped SnO₂ film as a counter electrode and 0.5M LiI/0.05 M I₂ in 1:1 acetonitrile-NMO (3-methyl-2-oxazolidinone) as the electrolyte solution. Illumination of the cell was performed with a calibrated Xe lamp and direct sun light. The illuminated cell area was 1 cm². Spectro-electrochemical (SEC)

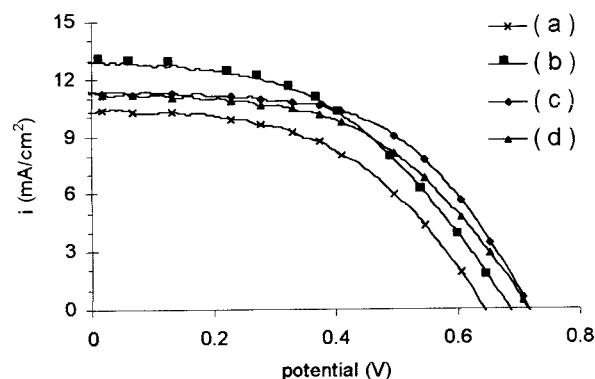


Figure 1. i - V curves of four DSSCs differing by the nanoporous electrodes used to fabricate them: the TiO₂ reference electrode, (a), and three bilayer electrodes (b-d). The Nb₂O₅ coating was made by 30 s dipping of a 6-μm TiO₂ matrix in 5-mM solution of NbCl₅ in dry ethanol, (b), Nb(isopropoxide)₅ in 2-propanol, (c), and Nb(ethoxide)₅ in ethanol, (d).

measurements were performed in a homemade Teflon cell three-electrode configuration. The measured nanoporous electrode served as an optical window and working electrode, Ag/AgCl served as a reference electrode, and a Pt wire functioned as a counter electrode. The electrolyte consisted of 0.2 M LiClO₄ in a pH 1.82 HClO₄ electrolyte solution, which was bubbled for 30 min with nitrogen to avoid oxygen. All the electrochemical measurements were performed using an Eco Chemie, model PGSTAT20 potentiostat.

Electrodeposition of Isolating Phenol Polymer on the Substrate. Electrodeposition of isolating phenol polymer was performed to block the pinholes on the conducting glass that supports the nanoporous TiO₂. An 85-mmol phenol, an 85-mmol tetra-butylammonium hydroxide (TBAOH), and a 40-mmol LiClO₄ in 25-mL dry ethanol was used as the electrolyte solution. The electrodeposition was conducted in a three-electrode electrochemical cell using Ag/AgCl as the reference electrode and Pt wire as the counter electrode. The potential of the nanoporous TiO₂ working electrode was scanned at 10 mV/s between 0 and +0.8 V versus Ag/AgCl up to 10 times, while the blocking of the substrate was reflected in the decrease of the polymerization current. After growth of the polymerization on the exposed substrate, the electrodes were sequentially rinsed with dry ethanol and deionized water (18.2 MΩ), dried at 120 °C for 30 min, and finally immersed in the dye solution.

Result and Discussion

Photoelectrochemical Characterization of Dye-Sensitized Solar Cells. Two types of nanoporous electrodes including standard TiO₂ and Nb₂O₅ coated ones are compared in this study. Figure 1 shows the i - V characteristics of four typical DSSCs that differ in their nanoporous electrodes. The cell shown in Figure 1a contained a standard nanoporous TiO₂ electrode, thus serving as a reference for the other three cells that contain bilayer electrodes. These three bilayer electrodes were prepared by dipping for 30 s in 5-mM solutions of different precursor solutions: NbCl₅ in dry ethanol (Figure 1b); Nb(isopropoxide)₅ in dry 2-propanol (Figure 1c); and Nb(ethoxide)₅ in dry ethanol (Figure 1d). The solar cell values summarized in Table 1 show that under one sun illumination, the Nb₂O₅ coating samples increase all cell parameters regardless of the coating solution. The best performance was achieved using the Nb(isopropoxide)₅ solution although the difference between the various coatings is minimal. For the best coating condition, the photocurrent increased from 10.2

(13) Zaban, A.; Aruna, S. T.; Gregg, B. A.; Mastai, Y. *J. Phys. Chem. B* **2000**, *104*, 4130.

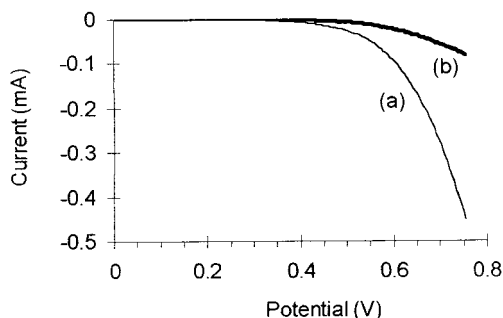
Table 1. The Solar Cell Parameters of the Cells Presented in Figure 1

sample	coating solution	efficiency (%)	Voc (mV)	Jsc (mA/cm ²)	ff. (%)	IPCE (%)
a	no	3.62	661	10.2	51.0	53.0
b	NbCl ₅ , 0.005 M, in ethanol	4.86	688	12.3	54.5	63.2
c	Nb(isopropoxide) ₅ , 0.005 M in 2-propanol	4.97	730	11.4	56.5	56.3
d	Nb(ethoxide) ₅ , 0.005 M in ethanol	4.49	730	10.7	54.7	54.3

Table 2. The Influence of Different Coating Methods on the Performance of the Solar Cells^a

sample	coating type	coating solution	ΔPmax (%)	ΔVoc (%)	ΔJsc (%)	Δff. (%)
1	spin 1 layer	NbCl ₅ /dry ethanol 0.24 M	30.0	13.7	-1.4	16.6
2	spin 5 layers	as above	22.5	8.8	-5.8	19.6
3	dip 30 s	as above	35.3	9.6	5.4	17.1
4	dip 150 s	as above	26.0	9.6	4.7	20.7

^a The parameters are presented as the increase percentage of the bilayer cells relative to the reference cell. The film thicknesses are approximately 5 μm.

**Figure 2.** Dark current vs applied bias of two cells containing the standard (a) and the bilayer (b) electrodes.

to 11.4 mA/cm², the photovoltage from 661 to 730 mV, and the fill factor from 51.0 to 56.5%. As a result, the conversion efficiency of the solar cell increased by 35% from 3.62 to 4.97%.

Table 2 presents the improvements achieved by various coating procedures using the NbCl₅ in dry ethanol solution. The data show that lengthy exposure or successive coatings do not improve the results. When we increased the dipping time longer than 5 min or number of coating over 10 layers, the electrodes became worse than the standard TiO₂ regarding DSSCs. We believe that this behavior results from partial blocking of the pores of the nanoporous electrode thus effecting the transport of the ions in the electrolyte. This finding is reflected in the decrease of the photocurrent and fill factors.

As suggested in our previous communication,¹¹ the improved cell performance achieved by the new bilayer electrode is attributed to the energy barrier formed by the deposition of the thin Nb₂O₅ layer. The Nb₂O₅ layer apparently decreases the recombination rate of the photoinjected electrons with the oxidized dye and ions in the electrolyte. In the following three sections, we will provide various proofs for the existence of such an energy barrier of ca. 100 mV above the TiO₂ conduction band. This work was performed using the electrodes prepared by dipping in the solution of Nb(isopropoxide)₅ in 2-propanol. As shown above, these electrodes provide the best coating.

Dark Current Measurements. Figure 2 shows the dark current of two cells containing the standard and the bilayer electrodes as a function of the applied potential. It also shows that throughout the measured potential range, the dark current of the bilayer containing cell is lower than that of the reference electrode. When testing the dark current of a porous system like

this one, it is important to ensure that the contribution of the substrate is minor. Although the surface area of the exposed substrate is much smaller than that of the porous semiconductor, this area can significantly affect the dark current when there is a big difference between the two materials concerning the kinetics of charge transfer to the electrolyte. To avoid any contribution from the exposed substrate, a thin layer of insulating polymer was deposited on the substrate after the formation of the electrode. The polymer layer consists of polyphenoxide of ca. 10 nm.¹⁴ This layer was electrochemically polymerized on the substrate areas that were not covered with a semiconductor.

Although the dark current in DSSCs is not a direct measurement of the recombination process, it can be used for the comparison of cells. Thus, the dark current presented in Figure 2 shows that one can expect a higher rate of recombination from the standard electrode in comparison with the bilayer one. This finding demonstrates that the coated Nb₂O₅ layer serves as a barrier at the electrode/electrolyte interface.

Spectro-Electrochemical Measurement. The applied potential-induced changes in the absorbance spectra of bare bilayer and standard electrodes were measured in acid solution (HClO₄, pH 1.82). The results presented in Figure 3 resemble similar measurements reported previously by others.^{15,16} The absorption intensity of both the standard electrode (Figure 3a) and the bilayer electrode (Figure 3b) increases at wavelengths that are longer than ca. 400 nm as the applied potential is scanned negatively. In addition, for both electrodes the negative potential induces a spectral bleach in the band gap region below ca. 400 nm. This phenomena was first reported by Liu and Bard with respect to CdS semiconductor film¹⁶ and subsequently by Fitzmaurice and co-workers regarding nanostructured TiO₂ (anatase) electrodes.¹⁷⁻²⁰ As pointed out by these researchers, the increase of the absorbance is assigned to the intra- and interband transition by electrons occupying

(14) Gregg, B. A.; Pichot, F.; Ferrere, S.; Fields, C. L. *J. Phys. Chem. B* **2001**, *105*, 1422.

(15) Boschloo, G.; Fitzmaurice, D. *J. Phys. Chem. B* **1999**, *103*, 3093.

(16) Liu, C. Y.; Bard, A. J. *J. Phys. Chem.* **1989**, *93*, 7749.

(17) O'Regan, B.; Gratzel, M.; Fitzmaurice, D. *Chem. Phys. Lett.* **1991**, *183*, 89.

(18) O'Regan, B.; Gratzel, M.; Fitzmaurice, D. *J. Phys. Chem.* **1991**, *95*, 10525.

(19) Redmond, G.; Fitzmaurice, D. *J. Phys. Chem.* **1993**, *97*, 1426.

(20) Rothenberger, G.; Fitzmaurice, D.; Gratzel, M. *J. Phys. Chem.* **1992**, *96*, 5983.

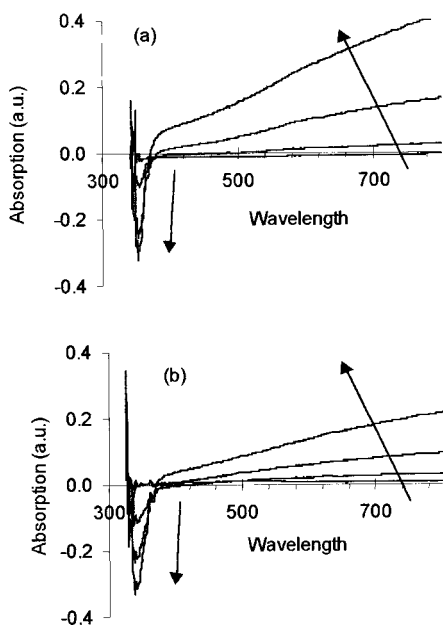


Figure 3. The absorbance change of the standard (a) and the bare bilayer (b) electrodes as a function of the applied potential in acidic solution (HClO_4 , pH 1.82). The applied potentials are 0, -0.4, -0.7, -0.8, and -0.9 V as indicated by the arrows.

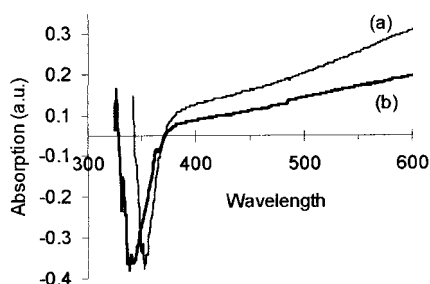
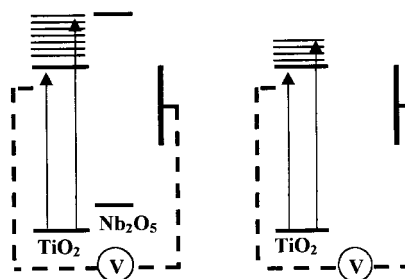


Figure 4. The absorbance change of the standard (a) and the bare bilayer (b) electrodes at -0.9 V vs SEC.

the conduction band states.²¹ The bleach of the gap region is accounted for by the apparent increase of the band gap energy that accompanies the conduction band filling with electrons.²² To compare the standard and bilayer electrodes, the absorbance changes of these electrodes at -0.9 V are plotted together in Figure 4. A comparison of the spectra in the range of wavelengths longer than 400 nm, especially in the region of near-infrared, shows that the conduction band electrons absorption in the Nb_2O_5 coated electrode is smaller than the absorption of bare TiO_2 . Also, the features of the spectra differ in the two electrodes. This spectral region was partly assigned to electrons localized in surface-state traps (Tiiv),²³ which may indicate that the Nb_2O_5 formed on the TiO_2 matrix effects these surface states.

In the region of band gap energy, the bleaching peak of the Nb_2O_5 coated electrode is wider than the peak of the standard electrode. This difference in width shows that the coated electrode can accumulate more negative states in the conduction band because of the energy barrier formed by the Nb_2O_5 layer (see Scheme 1). From

Scheme 1. The Expanding of the Bleaching Peak of the Coated Electrode to Shorter Wavelengths Indicates that the Nb_2O_5 Coating Enables Electron Accumulation to Higher Conduction Band States in Comparison with the Standard TiO_2 Electrode. The Coating Slows the Electron Reaction with the Solution



the change in width of the bleaching, we calculated approximately 100-mV difference between the highest occupied states of the bare and coated TiO_2 electrodes at -0.9V. This value correlates well with the literature value for the difference in conduction band potential of TiO_2 and Nb_2O_5 , 100 mV.¹² The results presented in Figures 3 and 4 further confirm that the reaction of the semiconductor electron with the electrolyte is slowed by this Nb_2O_5 coating.

Electrochemical Dye Desorption Measurement.

An electrochemical dye desorption experiment is a simple method to compare the potential distribution between different nanoporous semiconductor electrodes.²⁴ Although these measurements cannot provide quantitative information, they are important in enabling us to examine the quality of the Nb_2O_5 coating on the nanoporous TiO_2 film. We have shown previously that when a potential is applied to nanoporous electrodes, it does not distribute uniformly across the electrode.⁴ The applied potential appears next to the conducting substrate and decreases as the distance from the substrate increases. The potential decrease profile depends on the ratio between the conductivity of the semiconductor and the electrolyte that penetrates the pores.⁴ When an energy barrier is formed at the surface of the porous electrode, it is possible to accumulate more electrons in the semiconductor thus increasing its conductivity with respect to a noncoated analogue. The increased conductivity of the semiconductor should drive the potential distribution toward better uniformity. Thus, a comparison of the distribution of an applied potential provides information regarding the coating quality.

The electrodesorption experiment is based on the ability to desorb dye off the surface of the nanoporous electrode by negative potential. Thus, by scanning the potential negatively while measuring the change in dye concentration on the porous surface, one can obtain a value for the desorption window. For example, if the potential is distributed uniformly, all the dye should desorb within a narrow potential window. A nonuniform distribution can result in a desorption over a very wide range of voltages, up to hundreds of mVs.

Figure 5 presents a comparison between a standard TiO_2 electrode and a bilayer $\text{TiO}_2/\text{Nb}_2\text{O}_5$ electrode with

(21) Burstein, E. *Phys. Rev.* **1954**, *93*, 632.

(22) Paankove, J. In *Optical Processes in Semiconductors*; Dover Publications: New York, 1971.

(23) Finklea, H. In *Semiconductor Electrodes: Studies in Physical and Theoretical Chemistry 55*; Elsevier Science: Amsterdam, 1988.

(24) Kamat, P. V.; Bedja, I.; Hotchandani, S.; Patterson, I. K. *J. Phys. Chem.* **1996**, *100*, 4900.

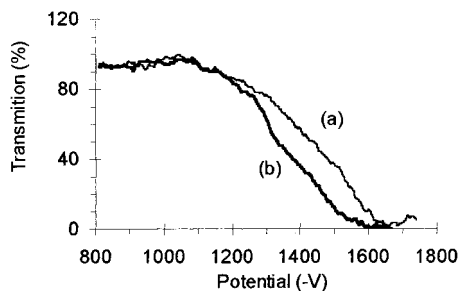


Figure 5. Dye electrodesorption from the standard (a) and bilayer (b) electrodes as a function of the applied potential.

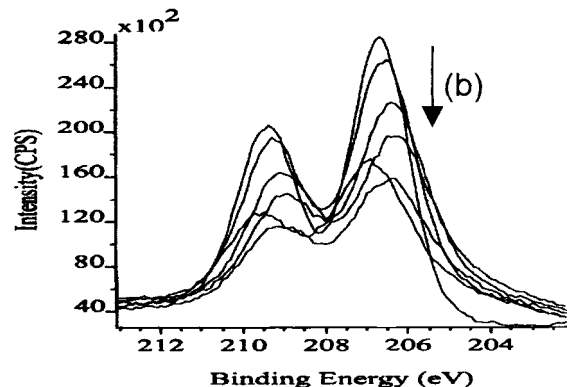
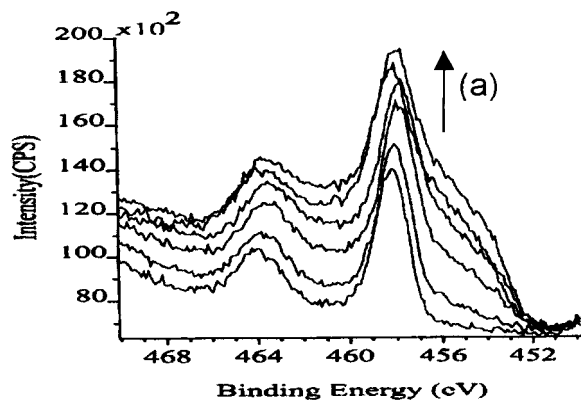


Figure 6. The XPS Ti 2p (a) and Nb 3d (b) peaks of the Nb₂O₅ coated TiO₂ electrode after different etching durations done by sputtering. The etching times are 3, 12, 17, 22, 27, and 34 min, as indicated by the arrows.

respect to the dye electrochemical desorption. The experiment was performed in a dry glovebox using a dry electrolyte to avoid water reduction. The electrochemical cell consisted of three electrodes: the working nanoporous electrode; Pt wire as a counter electrode, and Ag/AgNO₃ as a reference electrode. The cell was stirred throughout the experiment. Both the standard and bilayer electrodes of 4- μ m thickness were coated with N3 dye. For the desorption, the electrode potential was scanned between 0 and -1.8 V, at a scan rate of 5 mV/s. The desorption was measured by the transmission of the solution below the electrode at 500 nm, using monochromatic light and a photodiode. The transmission across the solution before the desorption and when all the dye desorbed off the electrode were set to 100% and 0%, respectively.

Scanning the potential negatively, the dye desorption started at ca. 1.1 V (100% transmission) when the electrode reached the sufficient negative potential. Beyond this threshold potential, the percentage of dye

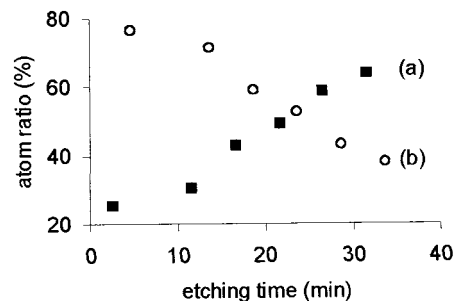


Figure 7. The atom ratio of Ti (a) and Nb (b) in the Nb₂O₅ coated TiO₂ film as a function of the X-ray etching time.

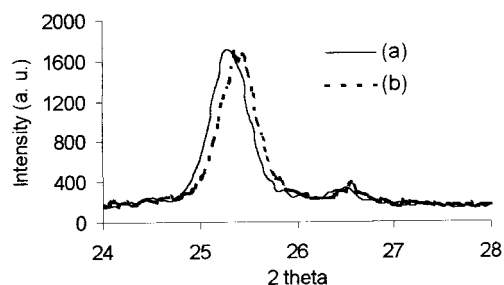


Figure 8. XRD of a TiO₂ film before (a) and after (b) Nb₂O₅ coating showing a small shift of the peaks' positions.

desorbed from the Nb₂O₅ coated electrode is higher than that of the reference electrode throughout the scan, that is, the transmission of the Nb₂O₅ coated electrode decreased 10–20% more than that of the reference electrode at any given potential. As mentioned above, dye desorbs when the effective potential reaches a threshold value. Figure 5 shows that the electrodesorption window is wider in the standard TiO₂ electrode. In other words, the noncoated TiO₂ electrode requires additional 100 mV negatively before the desorption potential is effectively present throughout the electrode. The results show that the Nb₂O₅ coating leads to a more uniform potential distribution across the electrode.

Morphology Measurement. X-ray photoelectron spectroscopy measurements were employed to estimate the thickness of the Nb₂O₅ coated layer. Using the Ti 2p and Nb 3d as the standards, we determined the ratio of the amount of Ti and Nb in the porous films. Figure 6 presents the change of XPS spectrum of Ti 2p (Figure 6a) and Nb 3d (Figure 6b) of the Nb₂O₅ coated TiO₂ film at different etching (by sputtering) durations from 3 to 32 min. As indicated after a longer time, the peak of Nb 3d decreased and that of Ti 2p increased. Figure 7 plots the atom ratio of Ti 2p and Nb 3d as a function of the etching time. It shows that the relative amount of Nb 3d decreases during the etching. This decrease is expected since the external part of the film is fully covered by Nb₂O₅, whereas after etching, a mixture of TiO₂ colloids and Nb₂O₅ coating are directly exposed to the XPS beam. It was impossible to determine the amount of Nb₂O₅ close to the substrate, since the etching is limited to a thickness less than 1 μ m. Therefore, we performed manual etching using adhesive tape and found that there is Nb₂O₅ adjacent to the conducting substrate.

The XPS results indicated that the Nb₂O₅ coating exists throughout the surface of the TiO₂ film. We understand that the niobium solution penetrates the porous TiO₂ film and that the niobium ions adsorb to

the surface of TiO_2 . After exposure to air and sintering, a layer of Nb_2O_5 is formed on top of the TiO_2 ; however, we have no data regarding the homogeneity of the coating. The thickness of the coated Nb_2O_5 layer could be estimated by performing calculation from the Ti/Nb atom ratio of the XPS results. Assuming that the TiO_2 particles are spherical and the coating is uniform, a layer of 2–3 nm was calculated.

X-ray diffraction was also employed to investigate the Nb_2O_5 coating. The diffractograms presented in Figure 8 show no sign of Nb_2O_5 because the coating is too thin to be detected. Moreover, the high-intensity peaks of the two materials overlap and cannot be resolved. However, the diffractograms were found to shift by ca. 0.1° because of the coating (Figure 8). This shift may indicate an epitaxial growth of the Nb_2O_5 on the TiO_2 ²⁵ as results from the good fit between unit cell axes of the two materials (a mismatch less than 2%).

Conclusions

A new kind of bilayer electrode for the dye-sensitized solar cell is reported. This new electrode consists of an

inner nanoporous TiO_2 matrix covered with a thin layer of Nb_2O_5 . The experimental evidence collected in the present study clearly show that the performance of the solar cells fabricated with the bilayer electrodes are superior to cells based on the standard single-material nanoporous electrodes. The results of dark current measurement, dye electrical desorption measurement, and spectro-electrochemical measurement suggest that an energy barrier is formed at the interface of electrode and electrolyte by the coated Nb_2O_5 layer. This energy barrier suppresses the recombination process and allows better potential distribution throughout the electrode.

Acknowledgment. We thank the Israel Science Foundation founded by The Israel Academy of Science and Humanities for supporting this research.

CM010343B

(25) Pashley, D. W. *Adv. Phys.* **1956**, *5*, 173.